Swage Hole Diameter Inspection using Hough Transform

Presented in 1st Data Storage Technology Conference (DST-CON 2008)

Orathai Suttijak[1], Sansanee Auephanwiriyakul[1] and Nipon Theera-Umpon[2]*

Abstract

In the quality control section of the hard disk drive industrials, one of the important tasks is the dimension measurement. One of the parts that are needed to be measured is a swage hole that has circular shape. Since an accurate measurement is needed, a microscope is used to capture the swage hole. In this paper, we utilized the Hough transform to measure the swage hole. To show the accuracy of the method, we compute the Hough transform on two different data sets, i.e., a synthetic data set and a real-world data set. The results show that the average error is 0.25 pixels for the synthetic data set whereas it is 6.66 micrometers for the real-world data set.

Introduction

NOWADAYS, hard disk drives (HDDs) is widely used as data storage. The compositions of an HDD are disk platters, spindle motor, and pivot arm. In the quality control section of the HDD manufacturing, one of the parts that is needed to be measured is the diameter of a swage hole of a pivot arm. In the present, the diameter inspection of a swage hole is done manually by human. The classification of a test pivot arm by a trained worker can be only "acceptation" or "rejection". The process cannot give the exact value of swage hole diameter. Moreover, the human inspection may cause some mistakes because of tiredness or inexpertness. The typical process of a quality control section is to randomly choose swage holes and measure them by a standard instrument. Therefore, some of defective swage holes may not be investigated which results in defective HDDs.

There are several research works on automatic measurement of objects. Yi et. al. used laser to measure the structure deformation for a large scale structure (Yi et al., 2000). Khan et. al. developed a system that capable of measuring the width, length, size, and shape of objects (Khan et al., 2005). This system is however unable to measure the rotate example. Huang et. al. used laser to measure the outer radius of run-out and taper (Huang et al., 2006). Kosmopoulos and Varvarigou developed a system to measure the width and depth of the door gap (Kosmopoulos and Varvarigou, 2001). The

[1]*Department of Computer Engineering, Faculty of Engineering Chiang Mai University, Thailand*

[2]*Department of Electrical Engineering, Faculty of Engineering, Chiang Mai University, Thailand*

**corresponding author; e-mail: sansanee@ieee.org; phone:6653942024; fax:6653942072*

error of this system was in the scale of millimeters. Some studies measured the inner and outer diameters of bearings by using CCD cameras (Lei L., 2004; Lei et al., 2005). Griffin and Villalbos proposed a new method for improving the efficiency of the automated quality control process (Griffin and Villalbos , 1992). They included the error values into the process capability zone.

In order to detect the circular part in a sample image, the edge pixels were processed through the Hough Transform method which calculated the location of the center and radius of a circle (Cooper and Cowan , 2004 ;Kerbyson and Atherton,1995; Yipet al., 1993; Philip et al., 1994). The detection of circles can also be achieved using a method based on the genetic algorithm (Ayala-Ramirez et al., 2006).

In this paper, we propose a method for measuring diameters of swage holes in pivot arms based on the Hough transform (HT.) The results from the HT indicate the center location (X_0, Y_0) and radius (r) of a circle. The diameter of swage holes are calculated and compared with actual values obtained from a standard instrument. To investigate the accuracy of the proposed method, we compute the Hough transform on two different data sets, i.e., a synthetic data set and a real-world data set.

This paper is organized as follows. Section II describes the proposed method and its related methods. The data sets and the results are presented in section III. The conclusion is drawn in section IV.

Methodology

There are two sets of images used in the experiments, i.e., a synthetic data set and a real-world data set. In case of the real-world data set, the images need to be processed through the median filtering to reduce spike noise. After noise reduction, the edges of the object are detected using the Canny edge detector. The edged image is then processed though the HT. The details of each step are described as follows.

A. Median Filtering

The median filtering is an effective method for image filtering. It is capable of removing noise, reducing, or enhancing the detail of an image. The median filter is well-known and more popular than the mean filter and the modal filter. It considers gray values in the neighborhood of a pixel and selects the median of these values as the output at the center pixel.

B. Canny Edge Detector

After we filter an image by the median filter, we applied the Canny edge detector to detect edges in the image (Canny, 1986). The Canny edge detection is optimal for step edges corrupted by white Gaussian noise. It is one of the best algorithms for edge detection consisting of 4 processes as follows:

1) Smoothing by Gaussian Filter

The image is smoothed by convolving the input image $I[i,j]$ with a Gaussian mask, i.e.,

$$S[i,j] = G[i,j,\sigma] * I[i,j], \qquad (1)$$

where * is the convolution operation. The Gaussian mask is defined as

$$G[i,j,\sigma] = \frac{1}{2\pi\sigma^2} e^{-(i^2+j^2)/2\sigma^2}, \qquad (2)$$

where σ is the spread of the Gaussian filter.

2) Gradient Calculation

The gradient of $S[i, j]$ can be computed using the gradient operators such as the Sobel. The partial derivatives of in the x-axis and y-axis can respectively be estimated as

$$P[i,j] = (S[i,j+1]-S[i,j]+S[i+1,j+1]-S[i+1,j])/2, \quad (3)$$

$$Q[i,j] = (S[i,j]-S[i+1,j]+S[i,j+1]-S[i+1,j+1])/2 \quad (4)$$

The magnitude and orientation of the gradient can respectively be calculated by

$$M[i, j] = \sqrt{P[i, j]^2 + Q[i, j]^2} \quad (5)$$

$$\theta[i,j] = \arctan(Q[i,j]/P[i,j]) \quad (6)$$

3) Nonmaxima Suppression

In this process, the nonmaxima suppression thins the ridge of the gradient magnitude $M[i,j]$. The result in this process is the thinned edges.

4) Double Threshold

The double threshold algorithm is used to detect and link the discontinuous edges by applying two thresholds to the nonmaxima suppression image.

C. Circle Detection using Hough Transform

Hough transform for circle detection is the calculation in three-dimensional parameter space (a,b,r). Consider the implicit equation of a circle,

$$(x_0 - a)^2 + (y_0 - b)^2 = r^2, \quad (7)$$

the parametric equations for a circle in the polar coordinate are

$$x = a + r\cos\theta, \quad (8)$$

$$y = b + r\sin\theta. \quad (9)$$

This method attempts to make a circle that is optimized with a set of points that are the edges in an image by using the accumulator array $M(a,b)$. In case of a circle with known radius, the HT in two-dimensional parameter space (a,b) can be expressed as follows

1) Specify the quantity of the parameter space for a and b.

2) Define the initial value for accumulator array $M(a,b)$.

3) Calculate a and b along the line where $0 < \theta < 360$ using

$$a = x - a = x - r\cos\theta, \quad (10)$$

$$b = y - r\sin\theta. \quad (11)$$

where x and y are the coordinate of the edge of the circle.

4) Increase the accumulator array $M(a,b)$ by 1.

5) When all edge points are calculated, the local maximum in the accumulator array is the center of the circle in the image.

In this research, the unknown parameters are a, b, and r. So we initialize the range of r for the HT method. The parameter set (a,b,r) that produces the maximum accumulator array $M(a,b,r)$ is selected to be the result of the HT.

Experimental Setup and Results

The data used in this research consist of two groups, i.e., a synthetic data set and a real-world data set.

A. Synthetic Data Set

In this experiment, we generate a set of synthetic circle images with random diameters and centers. We generate this synthetic data set to make sure that we have the ground truth. The data set

consists of 31 images. Each of them has the size of 720×576 pixels. The circle diameters are randomly set to 460 to 490 pixels. Table I shows the sample results from the HT of 6 synthetic images of circles with diameters between 466 to 471 pixels.

The results on all images are shown as a plot in Figure 1. We can see that the estimated diameters from the HT are very close to the actual diameters. The average error in this experiment is 0.25 pixels and the maximum error is 0.4 pixels. The results show that we cannot expect the perfect estimation. Even though an image is perfectly generated with strong and clear edge without noise, the error in the diameter estimation is still nonzero. This error is resulted from the spatial quantization of each pixel.

B. Real-World Data Set

We consider a set of images of circular-shape swage holes in pivot arms. These 720×576 pixels images are captured from a CCD camera through a microscope. The data set consists of 162 images from 81 swage holes. Two images are captured from each swage hole because there are two sides of the hole to be measured, i.e., the side with a serial number (C-side) and the opposite side of C (Off C-side). Because there is no ground truth of the diameters like in the synthetic data set, the estimated diameters from the HT are compared to the diameters measured from a smart scope which is a standard instrument.

Table 1. Sample Results of Synthetic Data Set from HT

Actual Diameter (pixels)	466	467	468	469	470	471
Diameter from HT (pixels)	465.6	467	467.8	468.6	469.8	470.6
Error	0.4	0	0.2	0.4	0.2	0.4

Table 2. Diameters of 4 Sample Swage Holes

	C-side			
Swage hole	1	2	3	4
HT diameter (μm)	2756.39	2758.71	2759.86	2759.86
Actual diameter (μm)	2758.44	2758.44	2755.9	2758.44
Error	2.05	0.27	3.96	1.42
	Off C-side			
Swage hole	1	2	3	4
HT diameter (μm)	2766.81	2759.86	2759.86	2766.81
Actual diameter (μm)	2758.44	2758.44	2755.9	2758.44
Error	8.37	1.42	3.96	8.37
Average error of 8 swage holes	3.7275			

Table 3. Error of Diameter Estimation of All Swage Holes

Data set	Diameter average error	
	C-side (μm)	Off C-side(μm)
1	11.05511	11.08243
2	3.780025	3.662302
3	3.461971	3.397404
4	6.384674	10.45486
Average error	6.170445	7.149249
Average error of 162 images	6.659847	

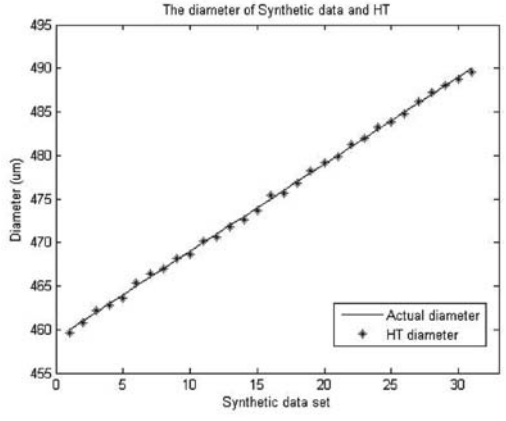

Figure 1. Comparison of the actual diameters of synthetic data and diameters from HT.

The data set consists of 4 subsets: 1) 21 swage holes before plating, 2) 20 swage holes from computer numerical control (CNC) machine, 3) 20 swage holes before plating, and 4) 20 swage holes after plating. Figure 2(a) shows a sample of the swage hole whereas Figure 2(b) is the edged image achieved by the Canny edge detection which will be fed into the HT to estimate the diameter.

Table 2 shows the diameters of 8 images from 4 swage holes. We can see that the estimated diameter using the HT is close to the diameters measured by a smart scope. The average error is 3.7275 micrometers. Table 3 shows the errors of all swage holes. The average errors of the C-side and Off C-side are 6.17 and 7.15 micrometers, respectively. The average error of all 162 images is 6.66 micrometers.

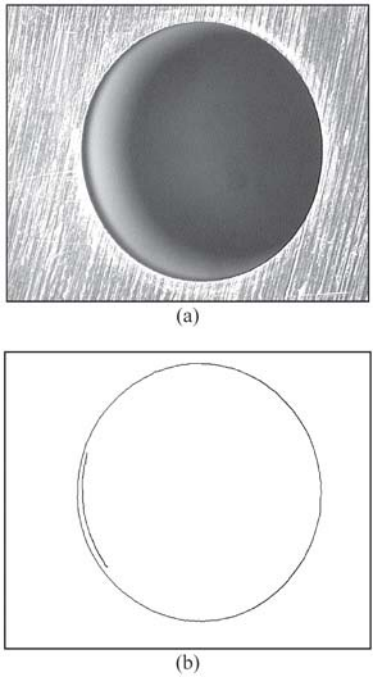

Figure 2. Sample of swage hole image (a) original image, (b) edged image

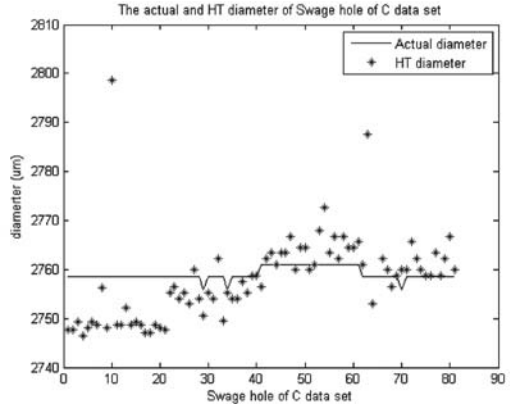

Figure 3. Comparison between the diameters on the C-side measured by the smart scope and the diameters estimated by the proposed method on the real-world data set.

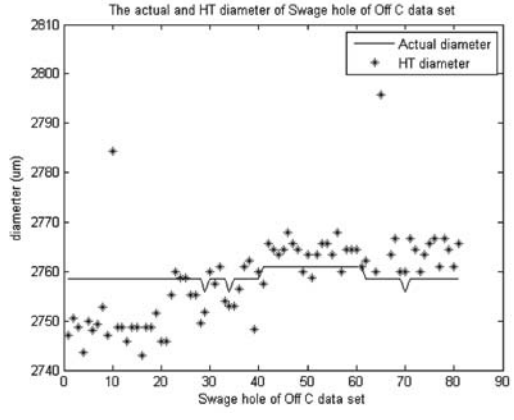

Figure 4. Comparison between the diameters on the Off C-side measured by the smart scope and the diameters estimated by the proposed method on the real-world data set.

To show the deviation of the estimated diameters, we show the results as plots shown in Figure 3 and 4. Figure 3 shows the comparison of the actual diameters and the diameters from the proposed method from the C-side. Even though most of the estimated diameters are close to the values measured from the smart scope, the maximum error is about 40 micrometers. Figure 4 also shows the comparison of the actual diameters and the diameters

from the proposed method, but from the Off C-side. Again, the most of the estimated diameters are close to the measured diameters from the smart scope. The high error occurs a few times with the maximum error of about 40 micrometers. This high error occurs in the image with the reflection from the light source. This problem causes the error in the edge detection step, and ultimately causes the error in the diameter estimation.

Conclusion

In this research, the Hough transform is applied to detect and estimate the diameter of a circle. It is applied to images from both the synthetic data and the real-world data set. In the synthetic data set in which the ground truth is available, the estimated diameters from the proposed method are very close to the actual diameters. The real-world data set contains 162 images of swage holes. The average error between the estimated diameters from the proposed method and the diameters measured by a smart scope is 6.66 micrometers. The high error occurs a few times in the estimation. They occur when the images have the reflection from the light source. This reflection causes the error in the edge detection, and ultimately causes the error in the diameter estimation. In the future, we will apply our method to measure a bore hole diameter of a pivot arm. A better edge detection algorithm will also be developed to be more robust to the light source variation.

Acknowledgment

This work was supported by the Hard Disk Drive Institute (HDDI) and the National Electronics and Computer Technology Center (NECTEC). We would like to thank Lanna Thai Electronic Components (LTEC) Ltd. for the valuable information and thankful cooperation during this research.

References

Ayala-Ramirez, V., Garcia-Capulin, C. H., Perez-Garcia, A., and Sanchez-Yanez, R. E. 2006. "Circle detection on images using genetic algorithms". *Pattern Recognition Letters*, vol. 27, pp.652-657.

Canny, J. 1986. "A computational approach to edge Detection," *IEEE Trans. on Pattern Analysis and Machine Intelligence*, vol.8, pp. 679-698.

Cooper, G. R. J., and Cowan, D. R. 2004. "The detection of circular feature in irregularly spaced data," *Computers and Geosciences*, vol. 30, issue. 1, pp. 101-105.

Griffin, P. M., and Villalbos, J. R. 1992. "Process capability of automated visual inspection systems," *IEEE Trans. Man and Cybernetics*, vol. 22, no. 3, pp. 441-448.

Hsieh, J. F. and Lin, P. D. 2007. "Application of homogenous transformation matrix to measurement of cam profiles on coordinate measuring machines". *International Journal of Machine Tools and Manufacture*, vol. 47, pp. 1593-1606.

Huang, C. K., Wang, L.G., Tang, H.C., and Tarng, Y.S. 2006. "Automatic laser inspection of outer diameter run-out and taper of micro-drills". *Journal of Materials Processing Technology*, vol. 171, no.2, pp.306-313 .

Kerbyson, D. J. and Atherton, T. J. 1995. "Circle detection using Hough transform filters," *Conf. of 5th Image Processing and its Applications*, pp. 370-374.

Khan, U. S., Iqbal, J., and Khan, M. A. 2005. "Automated inspection system using machine vision," *Proc of the 34th Applied Imagery and Pattern Recognition Workshop*.

Kosmopoulos, D., and Varvarigou, T. 2001. "Automated inspection of gaps on the automobile production line through stereo vision and specular reflection," *Computers in Industry*, vol. 46, no.1, pp.49-63.

Lei, L. 2004. "A Machine Vision System for Inspecting Bearing-diameter," *Proc. of the 5th World Congress on Intelligent Control and Automation*, Hangzhou, P. R. China, pp.3904-3906.

Lei, L., Zhou, X., and Pan, M. 2005. "Automated vision inspection system for the size measurement of workpieces," *Conf. on Instrumentation and Measurement Technology*, Ottawa, Canada, pp.872-877.

Philip, K. P., Dove, E. L., McPherson, D. D., Gotteiner, N. L., Stanford W., and Chandran, K. B. 1994. "The fuzzy Hough transform-feature extraction in medical images," *IEEE Trans. Medical Imaging*, vol. 13, issue. 2, pp. 235-240.

Yip, R. K. K., Leung, D. N. K., and Harrold, S.O. 1993. "Line segment patterns Hough transform for circles detection using a 2-dimensional array," *Int. Conf. on Industrial Electronics, Control, and Instrumentation*, vol. 3, pp.1361-1365.

Yi, Y., Li, Z., Li, X., and Deng, F. 2000. "Laser measurement for slight deformation of a large-scale structure," *Proc. of SPIE on Optical Measurement and Nondestructive Testing: Techniques and Applications*, vol. 4221, pp. 239-242.